ISSN: 2230-9926

Available online at http://www.journalijdr.com

IJDR

International Journal of Development Research
Vol. 08, Issue, 10, pp.23274-23282, October, 2018

ORIGINAL RESEARCH ARTICLE OPEN ACCESS

CHITOSAN FILMS DOPED WITH NANOPARTICLES OF METALLIC GOLD, SILVER, COPPER AND SILVER-PALLADIUM ALLOY A SKIN SUBSTITUTE

[1,*]Galo Cárdenas-Triviño, [2]Pamela Saavedra-Alvarez, [3]Luis Vergara-González, [4]Gerardo Cabello-Guzmán, [5]Javier Ojeda-Oyarzún and [6]Guillermo Solorzano

[1]Facultad de Ingeniería, DIMAD, Centro de Biomateriales y Nanotecnología, Universidad del Bío-Bío, Avda. Collao 1202, Concepción, Chile
[2]Facultad de Ciencia, Química y Farmacia, Universidad San Sebastián, Concepción, Chile
[3]Facultad de Ciencia, Departamento de Ciencias Biológicas y Químicas, Universidad San Sebastián, Concepción, Chile
[4]Facultad de Ciencia, Departamento Biología y Química, Universidad del Bío-Bío
[5]Facultad de Medicina Veterinaria, Universidad Austral de Chile, Valdivia, Chile
[6]Departamento de Engenharia Química e de Materiais, Pontifical Catholic University of Rio de Janeiro, R. Marquês de São Vicente, 225 Gávea, Rio de Janeiro - RJ, Brasil

ARTICLE INFO

Article History:
Received 25th July, 2018
Received in revised form
29th August, 2018
Accepted 18th September, 2018
Published online 29th October, 2018

Key Words:
Antibacterial Activity, Cutaneous Bacterial Infections, Chitosan, Metallic Nanoparticles, Liquid Chemical Deposition.

ABSTRACT

The antibiotic resistance increasing and the high rates of cutaneous bacterial infections on wounds and burns have attracted the development of new technologies. This study aimed to designing and evaluation of a medical dressing to use in skin infections and/or burns, from substances that have antibacterial activity such as chitosan and metallic nanoparticles (MNPs) of gold, silver, copper and silver/palladium alloy. The chemical liquid deposition (CLD) along with solvated metal atom dispersed (SMAD) method was used chitosan (QS) in 2-propanol, from which metallic nanoparticles (MNPs) ranging 10-50 nm of Cu, Au, Ag and Ag-Pd were obtained. The QS films with nanoparticles (NPs) characterization was carried out by techniques such as: X-ray dispersive spectroscopy (SEM / EDX), atomic force microscopy (AFM), high resolution transmission electron microscopy (HRTEM), Fourier Transform Infrared Spectroscopy (FT-IR) and Thermogravimetric Analysis (TGA). Assays were carried out to determine antibacterial activity films chitosan/nanoparticles using four bacterial strains (*E. coli, P. aeruginosa, S. epidermidis and S. aureus*), QS-Ag and Ag-Pd showed the best inhibitory action. Results obtained through bioassays in rats, showed a better reconstitution of the epithelium, less necrotic tissue and increase in vascularization, this study will aid to develop new materials with potential use in the formulation of dressings.

Citation: Galo Cárdenas-Triviño, Pamela Saavedra-Alvarez, Luis Vergara-González, Gerardo Cabello-Guzmán, Javier Ojeda-Oyarzún and Guillermo Solorzano, 2018. "Chitosan films doped with Nanoparticles of metallic gold, silver, copper and silver-palladium alloy a skin substitute.", *International Journal of Development Research*, 8, (10), 23274-23282.

INTRODUCTION

In order to decrease the frequency of skin infections, avoid resistance healing and healing of wounds, whether acute or chronic, post-traumatic, post-operative and Burns (Jiménez, 2008), it is recommended prophylaxis cleaning and protection of the wound from external environment.

Corresponding author: **Galo Cárdenas-Triviño,**
Facultad de Ingeniería, DIMAD, Centro de Biomateriales y Nanotecnología, Universidad del bío-Bío, Chile.

A dressing is an adequate element for healing of incisions, wounds, injured or diseased tissue; which can be elaborated by a wide variety of materials and aims to provide a favorable environment for healing of wounds. This element must promote hemostasis, protection, absorption and evaporation of fluids from the wound, reduce heat loss, eliminate the development microbial, promote autolysis, to support the compression to reduce swelling, provide support, reduce pain and bad smell, improve the appearance of the wound, and reduce overall costs associated with the treatment (Gennaro, 2003).

An ideal dressing must meet the following qualifications: possess antimicrobial activity, generate moisture absorption, be biocompatible and favor exudate absorption being easily removable without causing trauma to the wound. These ideal characteristics are attributed mainly to the functional properties of material, which help to heal wounds (Anjum *et al*., 2016). In any type of wound healing, it is essential to design a system of wound care, where antibacterial performance increases healing (Wang *et al*., 2012), being selection of materials very important. Several polymers have been studied with this purpose, as for example chitosan, alginate, cellulose, pectin and gelatin (Lin *et al*., 2013). An important property of chitosan is its antibacterial activity which is associated to protonation of amino groups in their units between glucosamine, however the exact mechanism by which the Chitosan and its derivatives possess this bactericide activity has not been clearly described. These include: the electrostatic interaction between the ammonia from the polycation and phosphoryl groups of the phospholipids present in the cell membrane of gram-negative bacteria, the presence of large size pores in cell membrane of Gram positive bacteria, the selective Chitosan interaction with traces of metals could inhibit toxins production and microbial growth. The chitosan bactericidal activity has been widely described by multiple authors; Hosseinnejad and Jafari (2016) indicate that the concentration of chitosan is directly proportional to its bactericidal activity. Regardless of which is the chitosan biocide action mechanism, there are different factors affecting the antimicrobial activity of this polymer such as:

- **pH effect:** chitosan more deacetylated (on a same length of chain) will have greater number of free amino groups to ionize at acid pH (pH < 6).
- **Molecular weight of chitosan:** there are three types of chitosan, high molecular weight, low molecular weight and oligosaccharides. According to multiple studies, each type of chitosan has a different bactericidal action mechanism and a spectrum of different action.

All applications of nanoparticles depend on physico-chemical properties, toxicity, size, surface properties and the type of nanomaterial synthesis. The Environmental Protection Agency (EPA) of United States has classified the nanoparticles depending on type of nanomaterials which are composed in: those based on carbon (Fullerene, graphene), those based on metals (metallic nanoparticles), dendrimers and nanopolymers, inorganic or non-metal, quantum dots, nanoclay and nanocomposites. Within them, metallic nanoparticles (MNPs) are which have aroused greater interest. Multiple studies have described effects biocides of Ag ions and compounds based on Ag in strains of *E. coli* (Wei *et al*., 2009), becoming Ag into a material widely used in the medicine field, being added to preparations as topical creams, sprays, antiseptic and tissues. A metal can be extremely toxic for most bacteria and yeasts to exceptionally low concentrations. The specific mechanisms that explain toxicity of metals are not fully clarified. However, depending on metal, biocide behavior can be caused by: (a) the reduction of metal potential and (b) the selectivity of metal atom donor (Palza, 2015). On the other hand, there are multiple properties that would explain toxicity of copper, among which are: the inhibition or alteration of bacterial protein synthesis, alteration in the permeability of cell membrane, causing the peroxidation, by inducing oxidative damage to lipids and imbalance of ions, sodium and potassium) and finally destruction or alteration of nucleic acids (DNA). It has been tested also palladium nanoparticles bactericidal action, stabilized in chitosan (Amarnath *et al*., 2012), it is estimated that the alloy silver palladium could present a synergism. According to those data reported, it was decided to propose a study based on nanoparticles of metallic gold, silver, copper and silver-palladium alloy stabilized on chitosan for a future dressing.

MATERIALS AND METHODS

Materials: QS (Mw 350 kDa, 95% deacetylated) was purchased from Quitoquímica Ltd (Coronel, Chile). 2-propanol was obtained from Merck SA. Au, Ag, Cu from Sigma-Aldrich (S. Louis, MO, USA). All reagents and solvents were reagent grade and used without further publication.

Methods

Synthesis of nanoparticles by chemical liquid deposition (CLD) and solvated metal atom dispersed (SMAD): Au, Ag, Cu, and Ag-Pd alloy nanoparticles were prepared by the method of chemical liquid deposition (CLD), which consists of physical deposition of metal vapors to 77 K (- 196,15° C). To perform the reaction is needed liquid nitrogen and a glass metal atoms reactor. The reactor has a source of metals evaporation, the crucible, composed of a tungsten basket coated with alumina (WAl_2O_3) that connects the ends of the electrodes (reaction of co-deposition requires between 30 and 40 Ampere (A)). Organic solvent it must be previously degassed three times by the freeze pump thaw procedure was also required using a glass device with 2-propanol. To achieve the reaction of co-deposition, an amount between 50-200 mg of metal is placed in the crucible to evaporate (Ag, Au, Cu and Ag-Pd), connects to the flask with the organic solvent, and is then evacuated the system until 5-10 bar which immerges the glass reactor in a 5 liters with liquid nitrogen Dewar. On the bottom of the reactor, 3.0 g of chitosan is placed. The crucible is heated slowly until the metal started to evaporate. The metal and the solvent is co-deposited for a period ranging from half to one hour, forming an array of freezing on the walls of the reactor, then stops heat slowly for half an hour. Once you complete this time, the reactor is filled with pure nitrogen gas and keep it with nitrogen flow stirring for 12 h at room temperature, then the composite is extracted by syphoning under vacuum with nitrogen atmosphere.

Elemental analysis SEM-EDX: X-ray elemental analysis was carried out using scanning electron microscopy equipment Hitachi Model SU3500. The analysis provided by the equipment allowed to determine the total content of carbon, hydrogen, nitrogen, sulfur and metals present. The determination of nanoparticles content, present on the surface of each film of chitosan doped with MNPs (NPs-Ag, NPs-Au, NPs-Cu and NPs-Ag-Pd).

High-resolution transmission electron microscopy (HRTEM): The transmission electron microscope of high resolution JEOL 2100F (200 kV), belonging to the laboratory of nanoscience and nanotechnology (LABNANO) of the Central Brazilian physical research (CBPF) or TEM JEOL 2010 (200 kV) belonging to the laboratory of nanostructured materials of the Pontifical University Catholic of Rio de Janeiro (PUC-RIO), allowed to obtain micrographs in order to determine range of nanoparticles size distribution as well as

the possible deformations and imperfections in the MNPs of Au, Ag, Cu and Ag-Pd-alloy.

Atomic Force Microscopy (AFM): The equipment to be used for analysis of atomic force is Digital Nanoscope IIIa, in operation of intermittent contact or Tapping mode. The sample analysis allowed to carry out an analysis of the surface of each film, identifying the presence of surfaces with more or less roughness between each nanoparticle film.

(FT-IR) Fourier transformed infrared spectroscopy: The equipment used to obtain spectra of IR, was Nicolet AVATAR 320. A software called Nicolet EZ OMNIC, which allowed to confirm the presence of the main organic groups present in the chitosan, the main links where MNPs joined this polymer and the presence of atomic groups of a same metal.

Thermogravimetric analysis (TGA): Thermogravimetric analysis was performed with equipment TGA Q50 V2010. The solid samples were deposited in the outer capsule of Platinum, and configure the equipment to warm them following a ramp of temperature of 10 °C/min up to 600° C, in nitrogen with 20 mL/min flow. The corresponding thermograms, calculating decomposition temperature and mass percent compositions of degradation products were determined.

Determination of antibacterial activity: Bacteriological assays were performed with four bacterial strains: *Escherichia coli* (ATCC25922), *Pseudomonas aeruginosa* (ATCC27853), *Staphylococcus aureus* (ATCC25923), and *Staphylococcus epidermidis* (ATCC12228). The antibacterial properties of MNPs supported in chitosan (QS) were assayed by a diffusion method. Briefly, a 1 cm^2 of QS film with the appropriate nanoparticle (MNPs) was deposited in a Mueller-Hinton (MH) agar Petri dish inoculated with the corresponding strain according with CLSI(10) standard recommendations. The antibacterial activity was determined by measuring inhibition zone from the edge of the chitosan film to the beginning of bacterial growth. All assays were incubated 24 hours at 35° C.

Test in rats: Bioassays in rats was carried out in the Institute of Sciences Veterinary belonging to Veterinary Hospital at Universidad Austral de Valdivia. Each rat had two wounds (1,5 cm^2) behind the neck. Then both wounds were inoculated with *E. coli* (10^8 ufc/mL). One of the wounds was dressed with a prepared of MNPs and the other wounds was treated with NaCl 0,9 % fluid. Then both wounds were covered with a bandage. After 14 days the wounds were evaluated macroscopically and taken biopsy samples for histopathological analysis. The analyses were repeated 3 times by each kind of nanoparticle. Both wound images were digitalized and the area of wound was calculated using the Klonk Image Measurement software. The results were analyzed by comparing differences in areas with untreated wounds. For evaluation of histopathological changes; a modified microscopic criterion adapted from Margulis (11) was assed. The reactive leukocyte infiltration and presence of necrotic tissues were assigned a severity grade of scale from 1 to 4, representing mild, moderate, severe and marked changes, respectively. For epidermis reconstruction

RESULTS AND DISCUSSION

Preparation of nanoparticles: Using method of chemical liquid deposition (CLD) were total different MNPs and each supplied Chitosan film presented at least two concentrations of metals. Metal concentrations per gram of polymer are described below in Table 1. Albarracín and Valderrama (2014) claim that the physical, chemical and antimicrobial properties of Chitosan films, are due to molecular interactions between these compounds and the polymer matrix modify the chemical compounds including. It is important to consider that the concentration of Chitosan films in MNPs can alter their antimicrobial properties, either increasing or decreasing its action, according to Kim (2007) bactericidal activity of QS-Ag film increases as increase silver concentration. The films that contain 1% by weight of Ag NPs show a maximum antibacterial activity that is why intended to determine the bactericidal activity of MNPs at different concentrations within the polymer matrix of Chitosan. See Table 1. Several concentration of NPs were obtained to test the bactericidal properties. According to Pinto (Pinto *et al*., 2012) there has been a growing interest in biocides materials. Thus, multiple studies including the appointed have been proposed to determine biocides properties of the NPs of silver on chitosan matrix. In this context, the main objective of this work was to elaborate and evaluate films of QS with MNPs of Au, Ag, Cu and Ag-Pd, which could function as a possible healing protective medical dressing with bacteriostatic properties in the application of skin infections or burns. With this objective, it was very important to characterize both properties of the film and MNPs present in it, through various methods, such as TGA, SEM, FTIR, HRTEM, this allows to determine the variables that can affect the activity of the film in tests *in vivo* or *in vitro*. Each film was made with at least two concentrations of different NPs this because according to Franci *et al*. (2015) there is a correlation between bactericidal effect, concentration and relationship between metal type, which dependent on the type of bacteria. Kim *et al*. (2007) for example, studied the antimicrobial activity of Ag NPs against *E. coli and S. aureus* showing that *E. coli* was inhibited at low concentrations, while inhibitory effects on the growth of *S. aureus* was less marked. That is why, it was, consider to develop films of at least two different concentrations for each metal.

Elemental analysis: The films elementary analysis, measured by dispersive X-ray spectroscopy (SEM/EDX), allowed to determination of the content of MNPs present on surface of each Chitosan film (QS-Ag, QS-Au, Cu-QS and QS-Ag/Pd), at different concentrations.

Table 1. Concentration of metal by film of chitosan in mg/g of polymer

Film	[M] mg/g polymer
QS-Au1	44
Qs-Au2	60
QS-Ag1	40
QS-Ag2	70
QS-Ag3	78
QS-Cu1	33
QS-Cu2	67
QS-Cu3	140
QS-Cu4	100
QS-Ag-Pd1	52.3
QS-Ag-Pd2	76.3

Table 2. Elemental analysis by scanning electron microscopy SEM-EDX (Scanning electron microscopy-energy dispersive X-ray spectroscopy)

Film	Metal composition (%)
QS-Ag1	0,34
QS-Ag2	0,77
QS-Ag3	0,19
QS-Au1	0,31
QS-Au2	1,55
QS-Cu1	0,24
QS-Cu2	0,87
QS-Cu3	0,41
QS-Ag-Pd1	0,93
QS-Ag-Pd2	2,95

Table 2 shows that in all the films analysed detected presence of metal surface. Furthermore, it was observed a correlation between MNPs concentration, present in the film at time of preparation and the percentage of MNPs present on each film surface, for example in films with Ag NPs case, it was observed that QS-Ag2 films presented a greater surface percentage of nanoparticles in contrast to QS-Ag1 and QS-Ag3films, this happens because NPs contented in these latest films were mostly absorbed by the polymer, which leads to a lower probability of oxidation. Elemental analysis of each film with dispersive X-ray spectroscopy (SEM/EDX) determined that films with higher percentage of metal surfacewereQS-Au2 and QS-Ag-Pd2 films, which leads to greater instability, tending to the agglomeration and oxidation of NPs present in the film. However, this instability is not reflected in thermogravimetric analysis.

(HRTEM) High-Resolution Transmission Electron Microscopy: Through HRTEM, were obtained images of QS-Ag, QS-Cu, QS-Au and QS-Ag-Pd films, where it was possible to determine morphology and size distribution of MNPs under studies, as well as also, to determine the presence or absence of distortions or imperfections that could be present at them, from an incomplete synthesis process.

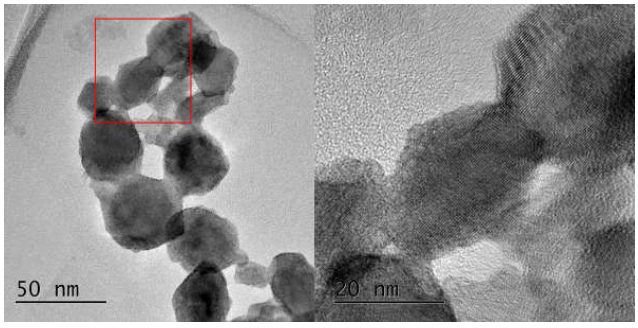

Figure 1b. TEM micrograph Chitosan-Ag NPs clear field

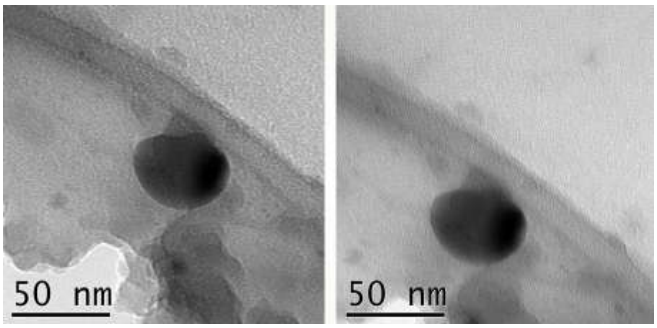

Figure1b. TEM micrograph Chitosan-Ag NPs clear field

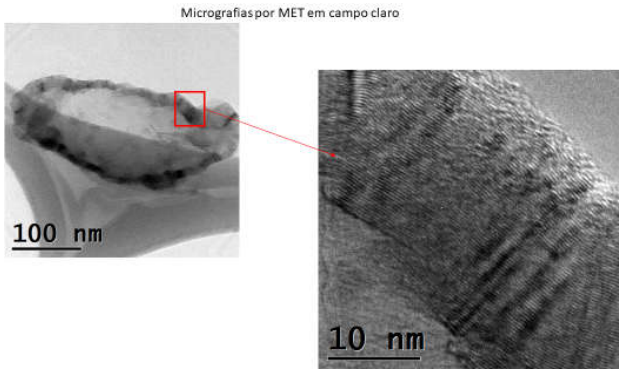

Figure 1c. HRTEM QS-AgPd. Average size 11,0 nm. Interplanar distance 0.33 nm

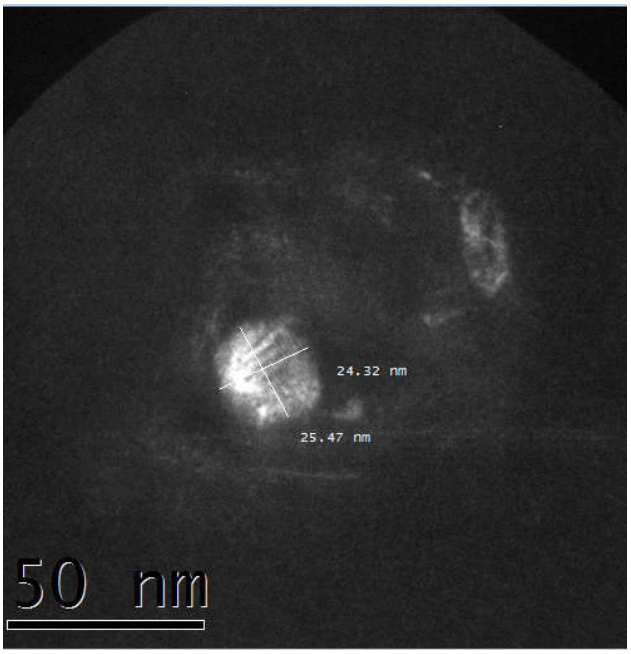

Figure 1d. HRTEM QS-Au. Average size 24.89 nm

Morphology and structure of MNPs: According to Viudez-Navarro (16), MNPs morphology was determined by laws of thermodynamics which establish that any material or system is stable only when it reaches the minimum state of Gibbs free energy. At nano level structures, this energy is reduced thus minimizing the surface. There are two ways to minimize energy, first one is to minimize surface, adopting a spherical shape, while the second one, minimizes surface energy by adopting the forms of different crystal facets. The thermodynamic equilibrium of a crystal is determined by the surface of each of its planes energy, there are three types of planes (111), (110) and (100), where it has been shown the most stable plane is (111). Regular metal nano particles are simple geometric arrangements, where the main structures are based on tetrahedrons, octahedrons and decahedra, formed from different types of crystal planes. In Figure 1a it is observed an octahedron and then in a higher magnification, the interplanar atoms distance is around 1 nm. Thus the Figure 1b shows a micrograph of clear field of QS-Ag3 film where it is possible to clearly see presence of a crystal of Ag, which apparently has shape of a cube octahedron. The Figure 1c is possible to see can single particles of 11,09 nm average size and 0.33 nm interplanar distance. Finally, in figure 1d it is observed single particles of 24.89 nm average size.

Table 3. Size distribution of metallic nanoparticles in the films

Nanoparticles present in the film	Size distribution range (nm)
QS-Ag1	16-32
QS-Ag2	15-20
QS-Ag3	15-36
QS-Cu-2	35-42
QS-Ag-Pd1	10-12
QS-Au	24-26

Table 4. AFM analysis of roughness and surface area of MNPs of Ag, Cu and Ag-Pd stabilized in Chitosan film

Films Film	Rq (nm)	Ra (nm)	Surface area $(\mu m)^2$
QS-Ag-Pd1	19,31	10,45	101,00
QS-Ag-Pd2	22,17	18,50	102,97
QS-Ag2	17,30	13,05	102,83
QS-Ag3	18,65	13,35	103,38
QS-Cu2	18,16	14,40	102,31
QS-Cu3	1,99	12,25	102,09

Table 5. Frequency bands of the main functional groups present in the chitosan and chitosan with metallic nanoparticles.

Characteristics Bands	Chitosan (cm^{-1})	QS-Ag2 (cm^{-1})	QS-Ag3 (cm^{-1})	QS-AgPd1 (cm^{-1})	QS-AgPd2 (cm^{-1})	QS-Au1 (cm^{-1})	QS-Au2 (cm^{-1})	QS-Cu2 (cm^{-1})	QS-Cu3 (cm^{-1})
Axial stretching -NH2 y -OH	3433,48	3445,07	3431,85	3434,02	3432,49	3415,68	3440,34	3366,51	3429,51
Axial stretching assymetric -CH2	2916,68		2916,39			2917,59			2913,29
Axial stretching symmetric C-CH2	2878,04	2874,63	2877,28	2878,55	2877,6	2869,96	2879,01	2876,5	2875,09
Stretching C=O primary amine	1650,09	1647,36	1653,55	1659,74	1649,93	1650,46	1650,23	1649,62	1644,27
Flexion amine I -NH	1600,84	1596,72	1598,09	1599,19	1600,23	1600,61	1597,3	1602,74	1600,82
Stretching amine III C-N	1331,65	1325,46	1322,37			1331,65	1327,96	1328,56	
Axial stretching symmetric CH2	1257,37	1258,95	1259,44		1257,81	1257,37	1253,66	1257,37	
Axial stretching symmetric C-O	1157,53	1157,19	1155,23	1158,32	1156,59	1158,32	1154,59	1156,21	1158,32
Stretching C6 of primary -OH	1092,74	1092,29	1089,51	1090,17	1092,13	1090,92	1091,99	1092,7	1091,33
Stretch C-C	713,5		663,09	656,9		656,9	658,11		
Stretch C-N		356,81	356,08	363,40	356,60	357,41	357,35	357,0	357,13

Table 6. Decomposition temperatures and weight loss of M-NPs stabilized in chitosan films

Films QS	Total Mass (mg)	Degradation temperature (°C) 337.9	Weight loss (%)	Weight loss (mg)
QS-Au1	6,414	313,82	66,09	4,239
QS-Ag3	6,053	314,74	66,27	4,012
QS-Ag2	7,737	314,71	60,21	4,658
QS-Ag1	4,533	312,34	62,29	2,823
QS-Cu3	5,646	314,84	68,23	3,852
QS-Cu2	5,671	313,08	62,09	3,521
QS-AgPd 1	8,832	314,99	59,18	5,227
QS-AgPd2	4,865	317,24	59,01	2,871

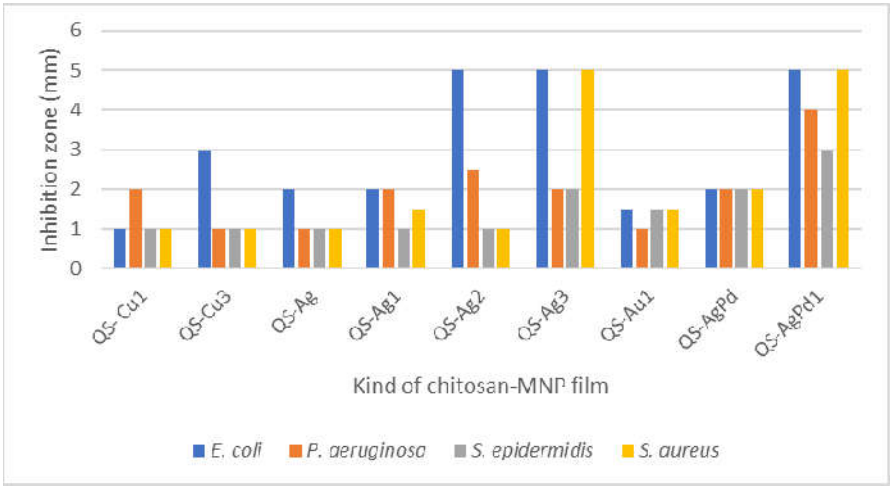

Figure 2. Inhibition zones of chitosan-MNPs films against the bacterial strains tested

Figure 3. A sequence of images showing the biopsy of rats subjected to two cuts, one control and one subject to cure in the presence of nanoparticles film and film of Chitosan

Size Distribution: From micrographs display, it was also possible to determine size of nanoparticles present in each film. Assuming MNPs are irregular, the size is an average of all of them, whereas the width and length of each one determines Ag, Au, Cu and Ag-Pd MNPs size distribution, present in chitosan films. In table 3 is observed as MNPs of Ag, Cu and Ag-Pd does not possess the same size range, mainly due to the type of metal and the amount of metal used in each case, for example, in case of QS-Ag1 and QS-Ag2 and QS-Ag3 films, have different size distribution of NPs, attributable to the amount of metal used in the synthesis of them and the variables involved in this process. According to Meléndrez (17) defrosting and type of solvent used in the synthesis by UNCCD reactions regulates nucleation process of nanoparticles, affecting size and structure of NPs, producing structures (icosahedron and cubeoctahedron, among others). It was observed distribution difference of sizes between NPs of a same metal. For example, in films of QS-Ag1 there are more than two NPs with equal size, which can be attributed to the different factors influencing the synthesis of nanoparticles. TEM results showed a size distribution of NPS, in which there is a distribution of sizes, different in each type of NPs in the film. Respect to the size of Ag NPs in QS-Ag1, QS-Ag2 and QS-Ag3 films it could be said that the Ag3 and Ag2 films have similar distribution size than QS-Ag1, or at least show presence of NPs Ag3 little bigger than the first one. According to Goyal (18) because that Ag NPs with diameters smaller than 20nm can bind to proteins that contain. Sulphur of bacterial cell membranes, would increase permeability of bacterial membrane causing the death of the bacteria.

Atomic force microscopy: Micrographs obtained by AFM analysis of films surface of MNPs stabilized in a matrix of QS, were obtained in three dimensions, allowing thereby a more complete analysis of the film surface behaviour, since, it is possible to obtain measurements of surface areas at three main levels x, y and z, identifying presence or absence of more or less roughness surfaces between each nanoparticle film. In table 4, Rq and Ra is represented the quadratic average roughness and roughness arithmetic mean respectively, which give a measurement of peaks nanometric achieved by the presence of roughness in the films.

According to table 4, films of QS-Ag-Pd, Ag-QS and QS-Cu increases its roughness when increases the concentration of nanoparticles, then films of QS-Ag-Pd2 have more roughness than films of QS-Ag/Pd1, the same QS-Ag3 film presents more roughness than QS-Ag2 film. Last QS-Cu films show a different tendency from the rest, showing greater roughness in QS-Cu2 films than films of QS-Cu3. Analyzing the roughness of all nanoparticles, films of QS-Ag-Pd showed greater Rq and Ra, where QS-Ag-Pd2 films presented higher roughness, with a Rq of 19.31nm and Ra of 18.50 nm. The characteristics of surface in contact with the injury, skin and dressing are important for effective healing and quality of patient life, since, application wound dressing with a surface softer and less rough is less painful and more biocompatible with the epithelial tissue formation, which indicate that the film application with less roughness as for example the QS-Cu3 film would be more biocompatible with the tissue at application time. Similarly, Cardenas (19) indicates that films Ra increases with the addition of MNPs, so films composed of QS and MNPs have a rougher surface. Nanometric high peaks allowed the films to more efficiently adhere to the surface of contact, as well as they would also generate an increase in the surface area which this cover, making this more effective use as a possible medical dressing bacteriostatic. QS-Ag-Pd2 film is the film with highest nanometric peaks and accordingly this one would be the film that has greater surface contact between the NPs and wound, thus reducing the healing time.

Infrared spectroscopy: Table 5 shows Infrared spectroscopy with Fourier transformed (FT-IR), where is possible to observe a summary about main absorption bands of MNPs from Spectra, which are succeeds in making the characterization of the structure of chitosan (QS) polymer from medium IR (up to 4000 cm^{-1}), in addition to corroborate the presence of polymer in each solid samples of NPs of Au, Ag, Cu and Ag-Pd alloy, starting from the which checks the presence of main organic groups present in the QS molecule. In the samples of MNPs spectra are presented in the far-IR away (up to 400 cm^{-1}), through which it is possible to distinguish the main links where the MNPs join this polymer and the presence of groups of a same metal.

Thermogravimetric Analyses (TGA): Thermogravimetric analysis aimed to demonstrated solids metal stability associated to temperature changes. Based on these results, it is possible to determine degradation temperature of Chitosan with MNPs and mass loss percentage samples had. Table 6 shows the thermogravimetric behaviour of chitosan film, showing presence of two thermal events, one at 66.7 °C and other thermal event at 337,9 °C, this is consistent with what was described by Zakaria *et al.* (2012), indicating that initial degradation of Chitosan occurs between 30 and 100° C. This degradation correspond to the loss of water absorbed or linked, while the second degradation temperature occurs at 210,8°C and continuous to 370,8°C, stage that corresponds to the degradation of Chitosan polymer; the maximum degradation temperature coincides with studies of different authors (Cárdenas (Cárdenas *et al*., 2008); Liu, (2013); González, (2000); Mishra *et al*. (2009); Zakaria, (2012)). Decomposition temperature analyses described in the annexes, are summarized in table 6, which shows that degradation temperature experimental average of QS with MNPs films is 314,5°C, with a percentage of mass loss average 62,09%, compared to the degradation temperature maximum of Chitosan being 337,9 °C, which indicates that metallic nanoparticles decrease the

thermal stability of Chitosan film. In addition, it is possible to observe that film's QS-Ag-Pd and QS-Cu-3, QS-Ag has the highest decomposition temperature, compared to the rest of the NPs, which demonstrates its high stability at high temperatures. Results obtained in the thermo gravimetric analysis, showed that thermal degradation of Chitosan-supported MNPs with an average of 314,47 °C, temperature considered lower than degradation temperature of the pure polymer. This is because the metal nanoparticles acts as impurity by lowering the temperature of decomposition of this one, increasing the entropy film.

Microbiological results: Microbiological results are summarized in Figure 2. Silver and silver-palladium film showed higher antibacterial activity than those with copper nanoparticles. The activity was different depending on microorganisms and concentration of nanoparticles in the film. As mentioned by Chen, (2012) the basal inhibitory activity showed by all films, may be due to the chitosan polymer or the organic acid used for solubilizing it. Regarding this Franci, (2015) indicated that while normally the size of nanoparticles between 1-100 nm, only particles with size below 30 nm where increases its bactericidal properties, because the ratio of surface area / volume increases. This would explain why in this study of QS-Ag2 and QS-Ag3 films show better activity than QS-Ag1. Similar situation was observed in QS-Cu case film, which according to HRTEM possess a size range between 35-42 nm, that in Kruk *et al*. (2015) studies show that 50 nm in average copper nanoparticles, were more active against Gram positive bacteria that the Ag NPs. However, the same study describes that NPs Cu has similar mechanism of action that NPs Ag what it would suppose that smaller NPs Cu, it would increase its antimicrobial activity, which would explain the low bactericidal activity in results. Respect to NPs forms, Franci *et al*. (2015) describes the activity of NPs Ag, which would not depend only on its concentration and size, but also on its shape. In this sense, *E. coli* seems to respond better to the triangular nanoparticles and is inhibited at low concentrations. Probably triangular shape gives a more positive charge to nanoparticles, which, together with the active faces on a triangular-shaped particle, is capable of ensuring greater activity.

The observed Ag NPs have cube octahedron, however, more comprehensive studies of the TEM micrographs are required to determine the presence of other forms of crystals already according to the surface area, the cube octahedron it has largest number of faces than triangular shape which would give it a larger surface area. With respect to the forms of NPs Cu, Au and Ag-Pd NPs is difficult to identify them since the micrographs obtained were not sufficiently clear to determine a definite shape. In addition, QS-Ag2 film presents a greater surface percentage of nanoparticles unlike the films of QSAg1 and QS-Ag-3, this is because this is because in these latest film NPs are mostly absorbed by the polymer then the composite is extracted by syphoning under vacuum with nitrogen atmosphere, which leads to a less likely to oxidize. The interaction of the MNPs of Au, Ag and Cu due to M-N (Metal-Amino) groups of chitosan is corroborated in FT-IR analyses. There is a decrease of the wavelength of absorption of the M-N due to the back bonding of electrons of nitrogen to the metal orbital. Also is proved by FT-IR, the presence of M-M (metal-metal) interactions existing in the far infrared, a clear duality of metallic particles is evident, showing the two forms, oxidized and not oxidized metal NPS. Microbiological results showed that the best inhibitory activity are displays by film QS-Ag3 and QS-AgPd1. Studies of Kim (2017), Franci (2015), Shameli *et al*., (2012) and Ruparelia *et al*. (2008), demonstrated and described the bactericidal activities of Ag NPs highlighting that factors such as size, shape and concentration of NPs affect the antimicrobial activity.

Animal tests: Regarding to bioassays conducted in rats, it was observed that rats that did not use film during the wound healing process, had better infiltration leukocyte, reconstitution of the epithelium, less tissue necrotic and fewer vessels connected throughout the dermis, respect to wounds treated with QS-MNPs films in 14 day studies. Goyal (29) declares that, while nanotechnology has proven to be promising, in topical applications, needs more studies that can relate dose and exposure of nanoparticles with penetration of nanoparticles and therapeutic efficacy. In addition, indicates that little is known about the mechanisms of transport of nanoparticles through the three main layers of skin and the effects it can have on patients. Another factor worth of mentioning is that results supplied, do not allow establishing a toxicological film in rats, since were not performed liver biochemical studies or other allowing establishing toxicity of MNPs and/or film.

Conclusion

Films of chitosan with at least two different concentrations of MNPs of Au, Ag, Cu and Ag-Pd prepared by chemical liquid deposition technique were synthesized. Each films was characterized and evaluated by different techniques. Thus the results of TEM and SEM allowed not only the presence of these MNPs in the film, but in the case of the HRTEM, to determine the size distribution of MNPs including in the films, ranging from 10-200 nm, in addition to its form in some cases as the shape of cube octahedron discovered in the NPs Ag. Thermogravimetric analysis provided information about the thermal behavior of the films, also found that incorporated MNPs do not lose the thermal behavior of the chitosan biopolymer and the average temperature of degradation of the elaborate QSMNPs films have an average degradation temperature of 314° C. Not only the presence of metal in the prepared films was determined by elemental analysis, they also show in surface percentage that varies between 0,19 to 2,95% in the films. The AFM micrographs gave values of Ra and Rq, which indicates that greater roughness is the surface area and adherence of the films to the wound. In this respect, the film QS-Ag-Pd2 with 19.31 Rq and a 10.45 Ra is which presented higher values. The areas of possible interaction metal-polymer was determined by FT-IR, within which the most noteworthy is the metal interaction with amine of chitosan polymer that is identified in the band located around the 3433,45 cm^{-1}. Furthermore, the bands in Far-IR around 356 cm^{-1} in all the films is due to the interaction of MNPs with chitosan nitrogen. The bacteriological tests performed allows us determining that the best inhibitory action is achieved with silver (QS-Ag3) and silver palladium alloy(QS-AgPd1) nanoparticles at the higher concentration used (78 and 76 mg of MNP/g chitosan). Both showed activity over Gram-negative and Gram-positive bacteria being the combination AgPd the most active. The bioassays in rats compared the degree of recovery of the skin exposed to film of chitosan with MNPs versus the degree of recovery of skin not exposed to films. In spite of this similar results at day 14, we detected particularly that chitosan MNPs rats have a decreased neutrophils count. This could be very

significant for wound healing process due to persistence influx of neutrophils cause more profound damages to the wound tissues, because neutrophils-derived toxic antimicrobial substances and proteases are not only for microbial pathogens but also for self-tissues (Ruparelia *et al*., 20018). On the other hand, at this concentration of MNPs toxicity is low because there is no change in alkaline phosphatase and levels of the enzymes ALT and GGT in biochemical analyses of liver in rats after 14 days of treatment.

Acknowledgement

The authors would like to acknowledge the funding support of Conicyt (Grant Fondecyt # 1140025) and to Quitoquímica Ltd, for laboratory facilities.

REFERENCES

Albarracín W. and Valderrama N. 2014. Modificaciones físicas, químicas y enzimáticas y sus efectos sobre las propiedades de las películas de quitosano. Revista Materia, 19(3), 301-312. http://dx.doi.org/10.1590/S1517-70762014000300013

Amarnath, K., Kumar, J., Reddy, T., Mahesh, V., Ayyappan, S. and Nellore, J. 2012. Synthesis and characterization of chitosan and grape polyphenols stabilized palladium nanoparticles and their antibacterial activity. Colloids and Surfaces B: Biointerfaces, 92 (1), 254-261. http://dx.doi.org/10.1016/j.colsurfb.2011.11.049

Anjum, S., Arora, A., Alam, M., & Gupta, B. 2016. International Journal of Pharmaceutics, 508(1-2), 92-101. http://dx.doi.org/ 10.1016/j.ijpharm.2016.05.013

Cárdenas, G., Diaz, J., Meléndrez M. and Cruzat C. 2008. Physicochemical properties of edible films from chitosan composites obtained by microwave heating. Polymer Bulletin, 61(1), 737-748. http://dx.doi: 10.1007/s00289-008-0994-7

Cárdenas, G., Diaz, J., Meléndrez, M., Cruzat C. and García, A. 2009. Colloidal Cu nanoparticles/chitosan composite film obtained by microwave heating for food package applications. Polymer Bulletin, 62(4),511-524.http://dx.doi: 10.1007/s00289-008-0031-x

Chen J. 2012. Effect of Molecular Weight, Acid, and Plasticizer on the Physicochemical and Antibacterial Properties of β-Chitosan Based Films, *Journal of Food Science*, 77(5),127-136. http://dx.doi: 10.1111/j.1750-3841.2012.02686.x

Clinical and Laboratory Standards Institute (CLSI). Performance standards for antimicrobial disk susceptibility test; approved Standards-Eleventh Edition. CLSI document M02-A11. Wayne, PA: Clinical and Laboratory Standards Institute; 2012.

Franci, G., Falanga, G., A., Galdiero, S., Palomba, L., Rai, M., Morelli, G., Galdiero M. 2015. Silver Nanoparticles as Potential Antibacterial Agents. Journal Molecules, 20(1), 8856-8874. http://doi:10.3390/molecules20058856

Gennaro, A., Remington A., J. and Belluci S. 2003. Remington Farmacia. Buenos Aires: Editorial Médica Panamericana

González, V., Guerrero, C., Ortiz U. 2000. Chemical structure and compatibility of polyamide-chitin and chitosan blends, Journal of Applied Polymer Science, 78 (4), 850-857. doi: 10.1002/1097-4628(20001024)

Goyal, R., Macri., L., Kaplan H. and Kohn, J. 2016. Nanoparticles and nanofibers for topical drug delivery. *Journal of Controlled Release,* 240 (1), 77-92. doi: 10.1016/j.jconrel.2015.10.049

Hosseinnejad, M. and Jafari S. 2016. Evaluation of different factors affecting antimicrobial properties of chitosan. International Journal of Biological Macromolecules, 85(1), 467-475. http://dx.doi.org/10.1016/j.ijbiomac.2016.01.022

Jiménez, C., C. 2008. Curación avanzada de heridas. Revista Colombiana de cirugía, 23(3), 146-155. http://www.scielo.org.co/pdf/ rcci/v23n3/v23n3a4.pdf

Kim, J.S., Kuk, E., Yu, K., Kim, J., Park, S., Lee, H., Kim, S., Park, Y., Hwang, C., Kim, Y., Lee, Y., Jeong, D., Cho M. 2007. Antimicrobial effects of silver nanoparticles. Nanomedicine: Nanotechnology, Biology and Medicine, 3(1) 95-101. http://dx.doi.org/10.1016/j.nano.2006.12.001

Kruk, T., Szczepanowicz, K., Stefanska, J., Socha, R., Warsznski P. 2015. Synthesis and antimicrobial activity of monodisperse copper nanoparticles. Colloids Surfaces B: Biointerfaces, 128 (1), 17-22. http://dx.doi.org/10.1016/j.colsurfb.2015.02.009

Lin, W.C., Lien, C.C., Yeh, J., Yu, C.M., S.H. Hsu, 2013. Bacterial cellulose and bacterial cellulose–chitosan membranes for wound dressing applications. Carbohydrate Polymers, 94 (1), 603–611. http://dx.doi.org/10.1016/j.carbpol.2013.01.076

Liu, Y., Liu, Z., Zhang, Y., Deng K. 2003. Graft copolymerization of methyl acrylate onto chitosan initiated by potassium diperyodate cuprate (III), Journal of Applied Polymer Science, 89 (8), 2283-2289. http://dx.doi:10.1002/app.12102

Margulis, A., Chaouat, M., Ben-Bassat, H., Eldad, A., Icekson, M., Breiterman S. and Neuman R. 2007. Comparison of topical iodine and silver sulfadiazine as therapies against sulfur mustard burns in a pig model.*Wound Repair and Regeneration*, *15*(6), 916-921. http://dx.doi:10.1111/j.1524-475X.2007.00316.x

Meléndrez, M., Cárdenas, G. and Arbiol, J. 2010. Synthesis and characterization of gallium colloidal nanoparticles. *Journal of Colloid and Interface Science,* 346(2), 279-287. http://doi:10.1016/j.jcis.2009.11.069

Mishra, D.K., Tripathy, J., Shirivastava, A., Pandey, P.K., Behari K. 2009. Synthesis and characterization of chitosan-g-methacrylic acid and studies of its additional physicochemical properties, such as swelling, metal-ion sorption, and flocculation behavior, *Journal of Applied Polymer Science,* 113(4), 2429-2439. http://dx.doi: 10.1002/app.29595

Palza H. 2015. Antimicrobial Polymers with Metal Nanoparticles. International Journal of Molecular Sciences, 16(1), 2099-2116. http://dx.doi.org/10.3390/ijms16012099

Pinto, R., Fernandes, S., Freire, C., Sadocco, P., Causio, J., Neto C. and Trindade, T. 2012. Antibacterial activity of optically transparent nanocomposite films based on chitosan or its derivatives and silver nanoparticles. Carbohydrate Research, 348(1), 77-83. http://dx.doi.org/10.1016/j.carres.2011.11.009

Ruparelia, J., Chatterjee, J., Duttagupta, K., Mukherji, SP., S. 2008. Strain specificity in antimicrobial activity of silver and copper nanoparticles. 4(3). 707-716. http://dx.doi: 10.1016/j.actbio.2007.11.006

Shameli, K., Ahmad, M.B., Jazayeri, S.D., Shabenzadeh, P., Sanpour, P., Jahangirian, H., Gharayebi Y. 2012. Investigation of antibacterial properties silvernanoparticles prepared via green method. *Chemistry Central Journal,* 6(1) 73. doi: 10.1186/1752-153X-6-73

Viudez-Navarro, A. J. 2011. Synthesis, Characterization and assembly of gold nanoparticles protected by molecular monolayers (Ph.D. chemistry thesis). Universidad de Córdoba, España. http://hdl.handle.net/10396/5536

Wang, T., X. Zhu, X. Xue, D. Wu, 2012. Hydrogel sheets of chitosan, honey and gelatine as burn wound dressings, Carbohyd. Polym. 88 (1), 75–83. Recuperado de: doi:10.1016/j.carbpol.2011.11.069

Wei, D.**,** Sun, W., Qian, W., Ye Y. and Ma X. 2009. The synthesis of chitosan- based silver nanoparticles and their antibacterial activity. *Carbohydrate Research,* 344(17), 2375-2382. http://dx.doi.org/10.1016/j.carres.2009.09.001

Wilgus, T. A., Roy S. and McDaniel J.C. 2013. Neutrophils and wound repair: positive actions and negative reactions. Advances in Wound Care, 2(7), 379-388). Doi: 10.1089/wound.2012.0383

Zakaria, Z., Izzah, Z., M. Jawaid and A. Hassan 2012. Effect of degree of deacetylation of chitosan on thermal stability andcompatibilityofchitosan-polyamideblend. Bioresources, 7 (4), 5568-5580. http://ojs.cnr.ncsu.edu/index.php/BioRes/article/view/BioRes_07_4_5568_Zakaria_ Deacetylation_ Chitosan_ Thermal_Stability/1808

****